



CHORUS

This is the accepted manuscript made available via CHORUS. The article has been published as:

Casimir Light in Dispersive Nanophotonics

Jamison Sloan, Nicholas Rivera, John D. Joannopoulos, and Marin Soljačić

Phys. Rev. Lett. **127**, 053603 — Published 29 July 2021

DOI: [10.1103/PhysRevLett.127.053603](https://doi.org/10.1103/PhysRevLett.127.053603)

Casimir light in dispersive nanophotonics

Jamison Sloan¹, Nicholas Rivera², John D. Joannopoulos², and Marin Soljačić²

¹ *Department of Electrical Engineering and Computer Science,*

Massachusetts Institute of Technology, Cambridge, MA 02139, United States

² *Department of Physics, Massachusetts Institute of Technology, Cambridge, MA 02139, United States*

Time-varying optical media, whose dielectric properties are actively modulated in time, introduce a host of novel effects in the classical propagation of light, and are of intense current interest. In the quantum domain, time-dependent media can be used to convert vacuum fluctuations (virtual photons) into pairs of real photons. We refer to these processes broadly as “dynamical vacuum effects” (DVEs). Despite interest for their potential applications as sources of quantum light, DVEs are generally very weak, presenting many opportunities for enhancement through modern techniques in nanophotonics, such as using media which support excitations such as plasmon and phonon polaritons. Here, we present a theory of weakly modulated DVEs in arbitrary nanostructured, dispersive, and dissipative systems. A key element of our framework is the simultaneous incorporation of time-modulation and “dispersion” through time-translation-breaking linear response theory. As an example, we use our approach to propose a highly efficient scheme for generating entangled surface polaritons based on time-modulation of the optical phonon frequency of a polar insulator.

The nonvanishing zero-point energy of quantum electrodynamics leads to a variety of observable consequences such as atomic energy shifts [1], spontaneous emission [2, 3], forces [4], and non-contact friction [5, 6]. A famously cited consequence of vacuum fluctuations is the Casimir effect [7–11], in which two uncharged bodies placed close together experience mutual attraction (or repulsion, in some cases [12–14]) due to electromagnetic field fluctuations. The character of any fluctuation-based phenomenon is determined by the electromagnetic modes around the structure of interest. As a result, the last two decades have provided promising insights about how nanostructured composites of existing and emerging optical materials can modify observable effects of zero-point fluctuations.

In time-varying systems, electromagnetic vacuum fluctuations can lead to the production of real photons. Famously, the “dynamical Casimir effect” predicts how a cavity with rapidly oscillating boundaries produces correlated photon pairs [15]. Other related phenomena include photon emission from rotating bodies [16], spontaneous parametric down-conversion in nonlinear materials [17], and cosmological phenomena [18–24]. The close connections among these phenomena are discussed in [25]. These “dynamical vacuum effects” (DVEs) have been studied in depth since the 1960s for their relation to fundamental questions about the quantum vacuum, and for their potential applications as quantum light sources [26–28]. Specifically, these processes are known to produce squeezed light (which is entangled if more than one mode is involved) [29, 30] which enjoys applications in quantum information [31], spectroscopy [32], and metrology [33].

Despite high interest, these DVEs are very weak, with the first direct observation of the dynamical Casimir effect occurring as recently as 2011 [34]. The strength of these effects can in principle be enhanced by nanostructured optical composites, and polaritonic materials with strong resonances, as has been seen with other fluctuation-based phenomena [2, 35, 36]. However, considering DVEs in such materials is complicated by the subtleties of optical materials which are simultaneously

dispersive and time-dependent. Largely due to this fundamental issue, there is not yet a general framework which describes these emission effects in arbitrary materials [37].

In this Letter, we present a theoretical framework, based on macroscopic quantum electrodynamics (MQED), which describes DVEs from weak modulations in arbitrary nanostructured, dispersive, and dissipative time-dependent media. This framework enables fundamental studies of DVEs in systems where time modulation frequencies are comparable to transition frequencies in dispersive materials. To exemplify these new theoretical capabilities, we show that phonon-polariton pairs can be generated on thin films of polar insulators (e.g., silicon carbide and hexagonal boron nitride), whose transverse optical (TO) phonon frequency is rapidly modulated in time. The high density of states (DOS) of surface phonon-polariton modes, in conjunction with dispersive resonances, leads to phonon-polariton pair generation efficiencies which are orders of magnitude higher than traditional parametric down conversion. These findings could enable experiments which generate a continuous spectrum of infrared surface polaritons.

There are inherent subtleties in describing the optical response of time-modulated dielectrics which are also dispersive. In systems where frequencies of time-modulation are far from any transition frequencies in the system, one can consider an “adiabatic” description of the time-dependent material. In this case, the permittivity can be taken as $\varepsilon(\omega; t)$, or simply $\varepsilon(t)$, as is done in many theoretical and experimental studies [38–44]. When the adiabatic approximation breaks down (e.g. in dispersive systems with similar modulation and transition frequencies), we must revert to the most general dielectric function allowed by linear response theory. In the absence of time-translation invariance, the polarization $\mathbf{P}(t)$ is connected to the applied field $\mathbf{E}(t)$ through a susceptibility $\chi(t, t')$. Consequently, the frequency response must be characterized by a two-frequency susceptibility $\chi(\omega, \omega') \equiv \int_{-\infty}^{\infty} dt dt' \chi(t, t') e^{i\omega t} e^{-i\omega' t'}$ [67]. The corresponding permittivity is $\varepsilon(\omega, \omega') = 2\pi\delta(\omega - \omega') + \chi(\omega, \omega')$, as illustrated

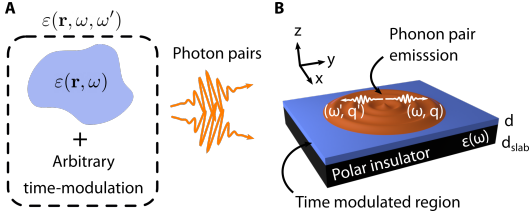


FIG. 1: **Photon pair emission from arbitrary time-dependent dielectric media.** (a) A dispersive dielectric $\varepsilon(\mathbf{r}, \omega)$ subject to an arbitrary time modulation can be described as having the more general dielectric function $\varepsilon(\mathbf{r}, \omega, \omega')$ which encodes both time dependence and dispersion. (b) A schematic of a thin film of polar insulator which has a small top layer which undergoes a time modulation. As a result, surface phonon-polariton pairs are produced with frequencies ω, ω' , and wavevectors q, q' .

in Fig. 1a. In this case, the displacement field \mathbf{D} is connected to the electric field \mathbf{E} as $\mathbf{D}(\omega) = \varepsilon_0 \int_{-\infty}^{\infty} \frac{d\omega'}{2\pi} \varepsilon(\omega, \omega') \mathbf{E}(\omega')$. We use this apparatus to parameterize the time-modulated materials we consider in our theory of DVEs. We consider a photonic structure (of arbitrary geometry and material composition), with a local dispersive dielectric function $\varepsilon_{\text{bg}}(\mathbf{r}, \omega)$. Then we impart some spatiotemporal change to the susceptibility $\Delta\chi(\mathbf{r}, \omega, \omega')$, so that the total permittivity is

$$\varepsilon(\mathbf{r}, \omega, \omega') = \varepsilon_{\text{bg}}(\mathbf{r}, \omega) [2\pi\delta(\omega - \omega')] + \Delta\chi(\mathbf{r}, \omega, \omega'). \quad (1)$$

Our theory of DVEs in systems described by the general form of Eq. 1 is based on a Hamiltonian description of electromagnetic field subject to interactions in general time-varying media. We use macroscopic quantum electrodynamics (MQED) [45, 46] to quantize the electromagnetic field in the background structure $\varepsilon_{\text{bg}}(\mathbf{r}, \omega)$. In this framework, the Hamiltonian of the bare electromagnetic field is $H_{\text{EM}} = \int_0^{\infty} d\omega \int d^3r \hbar\omega \mathbf{f}^\dagger(\mathbf{r}, \omega) \cdot \mathbf{f}(\mathbf{r}, \omega)$, where $\mathbf{f}^{(\dagger)}(\mathbf{r}, \omega)$ is the annihilation (creation) operator for a quantum harmonic oscillator at position \mathbf{r} and frequency ω . In such a medium, the electric field operator in the interaction picture is given as

$$\mathbf{E}(\mathbf{r}, t) = i\sqrt{\frac{\hbar}{\pi\varepsilon_0}} \int_0^{\infty} d\omega \frac{\omega^2}{c^2} \int d^3r' \sqrt{\text{Im} \varepsilon_{\text{bg}}(\mathbf{r}', \omega)} \times (\mathbf{G}(\mathbf{r}, \mathbf{r}', \omega) \mathbf{f}(\mathbf{r}', \omega) e^{-i\omega t} - \text{h.c.}). \quad (2)$$

Here, $\mathbf{G}(\mathbf{r}, \mathbf{r}', \omega)$ is the electromagnetic Green's function of the background which satisfies $(\nabla \times \nabla \times - \varepsilon_{\text{bg}}(\mathbf{r}, \omega) \frac{\omega^2}{c^2}) \mathbf{G}(\mathbf{r}, \mathbf{r}', \omega) = \delta(\mathbf{r} - \mathbf{r}') \mathbf{I}$, where \mathbf{I} is the 3×3 identity matrix. We assume that the permittivity change described by Eq. 1 creates a change to the polarization density $\mathbf{P}(\mathbf{r}, t)$, interacting with the electric field via $V(t) = -\int d^3r \mathbf{P}(\mathbf{r}, t) \cdot \mathbf{E}(\mathbf{r}, t)$ [17]. Then by relating the polarization to the electric field through linear response, we find the interaction Hamiltonian

$$V(t) = -\varepsilon_0 \int d^3r dt' \Delta\chi_{ij}(\mathbf{r}, t, t') E_j(\mathbf{r}, t') E_i(\mathbf{r}, t), \quad (3)$$

where we have used repeated index notation. When the permittivity change is small the electric field operator is well-approximated by that of the unperturbed field given in Eq. 2 (see S.I., which includes references [47–51]). Since almost all achievable time modulations of nanostructures are weak, this perturbative assumption poses little practical restriction on this formalism. To compute rates of two-photon emission, we consider scattering matrix elements that connect the electromagnetic vacuum state to final states which contain two photons. Taking the S-matrix elements to first order in perturbation theory (see S.I.), the probability P of two-photon emission is

$$P = \frac{1}{2\pi^2 c^4} \int_0^{\infty} d\omega d\omega' (\omega\omega')^2 \int d^3r d^3r' \times \text{Tr} [\Delta\chi(\mathbf{r}, \omega, -\omega') \text{Im} G(\mathbf{r}, \mathbf{r}', \omega') \Delta\chi^\dagger(\mathbf{r}', \omega, -\omega') \text{Im} G(\mathbf{r}', \mathbf{r}, \omega)], \quad (4)$$

where $\Delta\chi^\dagger$ is the matrix conjugate transpose of the tensor $\Delta\chi$ and $\text{Tr}[\cdot]$ denotes the trace. The Green's function encodes everything about background, and its imaginary part is closely related to the local DOS. Meanwhile, the tensor $\Delta\chi$ encodes everything about the imposed time dependence of the material.

As an example, our theoretical framework describes dispersion and loss in time-modulated thin films which generate pairs of entangled surface polaritons. Surface polaritons have enjoyed a myriad of applications due to their ability to maintain high confinement, and relatively low loss [52–55]. We specifically examine surface phonon-polaritons (SPHs) on thin films of the polar insulators silicon carbide (SiC) and hexagonal boron nitride (hBN). In the infrared, the dielectric response of polar insulators is well-described by the resonance of transverse optical (TO) phonon modes. The permittivity in this frequency range is given by the Lorentz oscillator $\varepsilon_{\text{bg}}(\omega) = \varepsilon_\infty + \omega_p^2/D(\omega)$ where ε_∞ is the permittivity at high frequencies, $D(\omega) \equiv \omega_0^2 - \omega^2 - i\omega\gamma$, ω_0 is the TO phonon frequency, ω_p is the plasma frequency, and γ is the damping rate. Phonon-polaritons are supported above the resonance at ω_0 , where $\text{Re} \varepsilon_{\text{bg}}(\omega) < -1$, which is referred to as the Reststrahlen band, or ‘‘RS band’’ (Fig. 2a).

To highlight the interplay between dispersion and time dependence in two-polariton spontaneous emission, we compare two different modulations of the polar insulator structures (Fig. 2b). The first is a nondispersive modulation, where a layer of thickness d has its index perturbed by a constant amount as $\varepsilon(t) = \varepsilon_{\text{bg}}(1 + \delta\varepsilon f(t))$. In this case, we have $\Delta\chi(\mathbf{r}, \omega, \omega') = \delta\varepsilon f(\omega - \omega')$ for $0 < z < d$, and 0 otherwise. In this expression, $f(\omega)$ is the Fourier transform of the modulation profile. If the change in index is caused by a nonlinear layer with $\chi^{(2)} = 100$ pm/V, then an electric field strength of 10^7 V/m gives $\delta\varepsilon = 10^{-3}$. The second is a dispersive modulation, where over a thickness d , the transverse optical phonon frequency ω_0 is modulated to deviate from its usual value as a function of time as $\omega_0^2 \rightarrow \omega_0^2(1 + \delta\omega f(t))$.

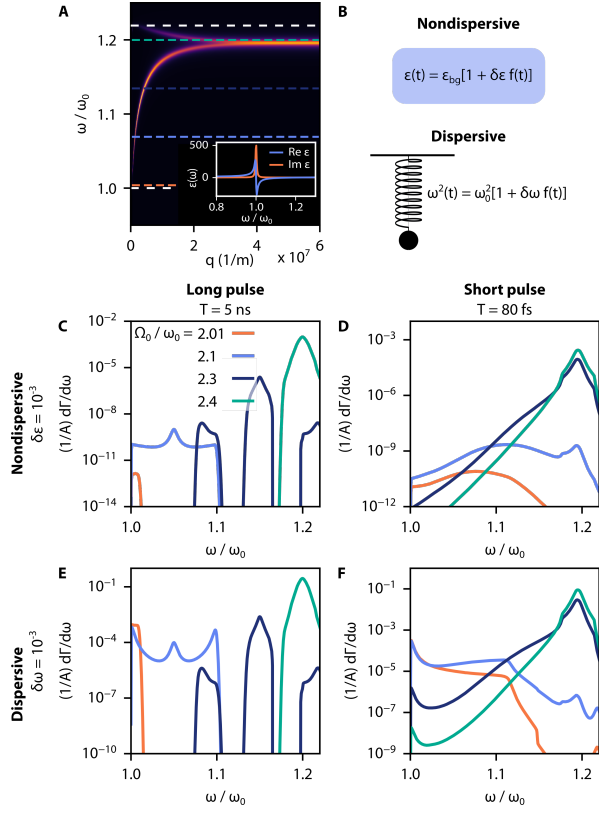


FIG. 2: Dynamical Casimir effect for silicon carbide phonon-polaritons. (a) Dispersion relation of phonon-polaritons on $d_{\text{slab}} = 100$ nm thick slab of SiC. Dashed lines mark the edges of the RS band. Inset shows the Lorentz oscillator permittivity around $\omega_0 = 1.49 \times 10^{14}$ rad/s. (b) Schematic representation of nondispersive time modulations of the permittivity, versus dispersive modulations of the transverse optical phonon frequency ω_0 . (c-f) Differential rate per unit area $(1/A)d\Gamma/d\omega$ for phonon-polariton pairs production for various values of $\Omega_0/\omega_0 = \{2.01, 2.1, 2.3, 2.4\}$, as well as short ($T = 80$ fs) and long ($T = 5$ ns) pulses. The modulated region is assumed to be $d = 10$ nm thick. Panels (c, d) show a nondispersive modulation with $\delta\varepsilon = 10^{-3}$. Panels (e, f) show a dispersive modulation with $\delta\omega = 10^{-3}$.

In this case, $\Delta\chi(\omega, \omega') = \delta\omega \omega_0^2 \omega_p^2 f(\omega - \omega') / (D(\omega)D(\omega'))$ to first order in $\delta\omega$ (see S.I.). From the experimental models presented in [56] for SiC, we estimate that an applied field strength of 1 GV/m gives rise to a frequency shift of the order $\delta\omega = 10^{-3}$. We will compare the two modulation types with the same fractional change in parameter $\delta\varepsilon = \delta\omega = 10^{-3}$ to highlight that around ω_0 , a fractional change $\delta\omega$ causes much stronger effects than $\delta\varepsilon$. Later, we comment on efficiencies given the same applied field strength.

We modulate the surface layer with perturbations of the form $f(t) = \cos(\Omega_0 t) e^{-t^2/2T^2}$. This enables us to consider modulations across many timescales, from ultrashort pulses, to nearly monochromatic (CW) modulations. Applying our formalism to the geometry depicted in Fig. 1b, we find that the probability of two-polariton emission per unit frequency

ω and ω' is given as

$$\frac{1}{A} \frac{dP}{d\omega d\omega'} = \frac{|\Delta\chi(\omega, -\omega')|^2}{16\pi^3} \int_0^\infty dq q (1 - e^{-2qd})^2 \times \text{Im } r_p(\omega, q) \text{Im } r_p(\omega', q). \quad (5)$$

Here, $r_p(\omega, q)$ is the p-polarized reflectivity associated with the interface, and A is the sample area [68] Equation 5 encodes the frequency correlations between the two emitted quanta ω and ω' . Once $\Delta\chi$ is chosen, Eq. 5 can be integrated over ω' and normalized by the pulse duration as $\Gamma \equiv P/T$ to obtain an area-normalized rate per frequency $(1/A)d\Gamma/d\omega = (1/AT) \int_0^\infty d\omega' dP/d\omega d\omega'$. This quantity represents the emission rate which is detected classically at frequency ω , and thus no longer discriminates between the two photons of the emitted pair.

We obtained results for SiC which is modulated both dispersively and nondispersively. Fig. 2a shows the phonon-polariton dispersion for a 100 nm layer of SiC (dielectric parameters taken from [57]). Figs. 2c-f show the corresponding rate distribution $(1/A)d\Gamma/d\omega$ for each of the marked modulation frequencies. For a long pulse (Fig. 2c), the two polaritons obey an energy conservation constraint $\omega + \omega' \approx \Omega_0$. In this regime, the behavior of the rate spectrum $d\Gamma/d\omega$ is determined by where $\Omega_0/2$ lies in the RS band (see dashed lines on Fig. 2a). For various Ω_0 , the spectra are symmetrically peaked around $\Omega_0/2$, with widths set by the loss. The strongest response occurs around $\Omega_0/\omega_0 = 2.4$ where the DOS of SPhPs is highest. At the slightly lower excitation frequency $\Omega_0/\omega_0 = 2.3$, the central peak at $\Omega_0/2$ is flanked by two symmetrical side peaks. These secondary peaks occur since $\Omega_0/2$ lies in between two bands of the dispersion, and thus one possibility for satisfying the approximate energy conservation relation is that one polariton is emitted into each band at the same wavevector q . Also notably, the modulation associated with $\Omega_0/\omega_0 = 2.01$ produces very little response, owing to the low DOS at the bottom of the RS band. For a short pulse (Fig. 2d), the general trend in magnitudes between the excitation frequencies is the same. Additionally, since a short pulse eliminates the strict energy conservation condition, polaritons are emitted at many frequency pairs. As a result, the shape of the spectrum for most excitation frequencies is peaked near the top of the RS band where the DOS is highest.

For dispersive modulations, many aspects of SPhP pair production remain the same. However, several key changes emerge as a result of the difference in the factor $|\Delta\chi|^2 \propto 1/|D(\omega)D(\omega')|^2$, which becomes large when $\omega, \omega' \approx \omega_0$. This condition corresponds to parametric resonance of phonons which dictate the dielectric response. While the behavior of the monochromatic modulation (Fig. 2e) for higher frequencies Ω_0 remains qualitatively the same, the magnitudes of the peaks for $\Omega_0/\omega_0 = 2.1, 2.01$ increase substantially. Interestingly, for $\Omega_0/\omega_0 = 2.1$, this resonance amplifies frequency distribution tails, so that nondegenerate pair production is actually slightly preferred. For short pulses (Fig.

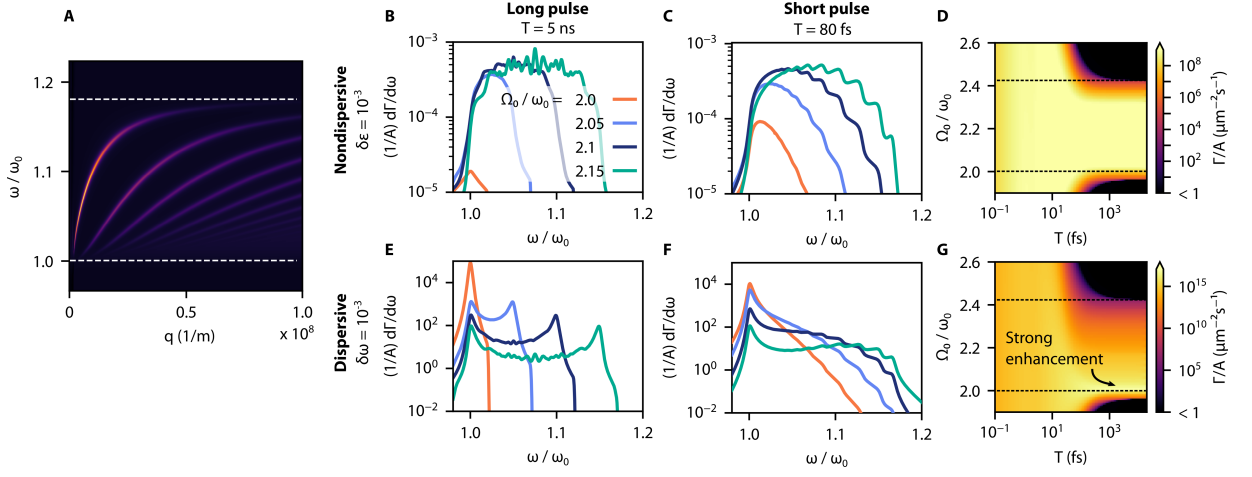


FIG. 3: **Achieving strong DVEs through dispersive modulations.** (a) Dispersion of surface phonon-polaritons on a thin layer of hBN ($d_{\text{slab}} = 100$ nm) in the upper RS band ($\omega_0 = 2.56 \times 10^{14}$ rad/s). (b, c) Differential rate per unit area $(1/A)d\Gamma/d\omega$ for phonon-polariton pairs production for various values of $\Omega_0/\omega_0 = \{2, 2.05, 2.1, 2.15\}$, as well as short ($T = 80$ fs) and long ($T = 5$ ns) pulses. (d) Total emission rate per area of phonon-polariton pairs as a function of pulse duration T and frequency Ω_0 . (e-g) Same as (b-d), except that the modulation is dispersive. Panel (g) shows the strong enhancement which occurs for monochromatic modulations when $\Omega_0/\omega_0 = 2$, corresponding to enhancement of DVEs by dispersive parametric amplification.

2f), the DOS behavior remains largely unchanged. However, distribution tails at the bottom of the RS band near ω_0 are raised, in contrast to the nondispersive behavior (Fig. 2d). There are two main factors which may cause strong enhancement of the phonon emission spectrum: high DOS, and parametric resonance around ω_0 . For SiC, these large dispersive enhancements occur around ω_0 , which is actually at a point of very low DOS in the dispersion. We can then reason that the strongest emission should come from systems where the dispersive resonance overlaps more strongly with the high DOS.

To this end, we elucidate how SPhPs on hBN, due to their multi-banded nature, can enjoy much stronger enhancement through dispersive modulations. Unlike SiC, hBN is an anisotropic polar insulator, with different transverse optical phonon frequencies in the in-plane or out-of-plane directions. As a result, hBN has two RS bands, and the dispersion relation is hyperbolic and multi-branched in each RS band [55]. The dispersion relation in the upper RS band of thin hBN is seen in Fig. 3a (dielectric parameters taken from [58, 59]). In contrast to SiC, the DOS of SPhPs is spread broadly across the upper RS band. Figs. 3b,c show the emitted pair spectrum for a variety of driving frequencies, similarly to SiC. Fringes in the emission spectra are a direct consequence of interference among the many ways two PhPs can distribute themselves into dispersion branches. Fig. 3d shows the total emission rate integrated over the upper RS band for various modulation frequencies Ω_0 and pulse durations T . Due to the relatively even DOS, the nondispersive emission rate is relatively uniform ($\Gamma/A \approx 10^9 \mu\text{m}^{-2}\text{s}^{-1}$) across a wide range of parameters.

For a dispersive modulation, the strongest emission occurs for degenerate production around ω_0 when the system is modulated at $2\omega_0$. Around this point (Fig. 3g), the emis-

sion rate is orders of magnitude higher than for long pulses outside of the resonance around ω_0 . Even though achieving $\delta\varepsilon = 10^{-3}$ through a nonlinear substrate requires a lower applied field than a TO phonon frequency shift of equivalent proportion, the sensitive nature of the dispersive modulations provides opportunities for improved efficiency. We estimate that with an applied field strength of 1 GV/m, the nondispersive modulation achieved through a thin nonlinear ($\chi^{(2)} = 100$ pm/V) layer has a quantum efficiency of the order $\eta \approx 10^{-9}$, while at the same field strength, the dispersive modulation has $\eta \approx 10^{-5}$. Given that evidence of parametric amplification of optical phonons in SiC has already been demonstrated [56], we believe that efficient generation of SPhP pairs on SiC and hBN by optical excitation should be feasible. We have also applied our formalism to the generation of graphene plasmons on a nonlinear substrate, and found this process could have an efficiency $\eta \approx 10^{-4}$ (see S.I., which includes references [60–62]). Such efficiencies could exceed the highest seen for pair generation to date [63].

To generate surface polaritons experimentally, the chosen material could be irradiated with strong laser pulses. Then, grating couplers could be etched into the substrate so that a fiber probe can receive the emitted light before polaritons are attenuated. For quantum experiment, the fibers would be directed toward a detection setup which measures the quantum correlations of the two-photon state. It may also be possible to measure the two-photon interference fringes which emerge in the classical radiation distribution (e.g., Fig. 3b, e). Such an observation could provide indirect evidence of entangled pairs, even if a quantum correlated detection scheme is difficult to achieve.

In summary, we have presented a Hamiltonian theory which governs photon interactions in dispersive time-dependent di-

electrics. Our work shows that the role of dispersion is critical in describing and enhancing these phenomena, as we showed for time-modulated polar insulators. Our framework is amenable to design and optimization of complex structures for experiments and potential devices. Beyond this, the Hamiltonian MQED formalism we have presented can enable further studies of light-matter interactions in arbitrary time-dependent materials. For example, one could model how spontaneous emission and energy-level shifts of quantum emitters are modified via time-modulation. Finally, this formalism could provide opportunities for studying the role that parametric amplification of quasiparticles can play in exotic effects in solid-state systems such as light-induced superconductivity [64, 65]. Broadly, we anticipate that our framework will describe phenomena in many timely experimental platforms featuring ultrafast optical modulations.

The authors thank Yannick Salamin and Prof. Ido Kaminer for helpful discussions. This material is based upon work supported by the Defense Advanced Research Projects Agency (DARPA) under Agreement No. HR00112090081. This work was supported in part by the U.S. Army Research Office through the Institute for Soldier Nanotechnologies under award number W911NF-18-2-0048. J.S. was supported in part by NDSEG fellowship No. F-1730184536. N.R. was supported by Department of Energy Fellowship DE-FG02-97ER25308.

-
- [1] H. A. Bethe, *Physical Review* **72**, 339 (1947).
 [2] E. Purcell, *Phys. Rev.* **69**, 681 (1946).
 [3] J.-M. Gérard and B. Gayral, *Journal of lightwave technology* **17**, 2089 (1999).
 [4] S. K. Lamoreaux, *Physical Review Letters* **78**, 5 (1997).
 [5] M. Kardar and R. Golestanian, *Reviews of Modern Physics* **71**, 1233 (1999).
 [6] J. Pendry, *Journal of Physics: Condensed Matter* **9**, 10301 (1997).
 [7] U. Mohideen and A. Roy, *Physical Review Letters* **81**, 4549 (1998).
 [8] G. Bressi, G. Carugno, R. Onofrio, and G. Ruoso, *Physical review letters* **88**, 041804 (2002).
 [9] G. Klimchitskaya, U. Mohideen, and V. Mostepanenko, *Reviews of Modern Physics* **81**, 1827 (2009).
 [10] M. Bordag, U. Mohideen, and V. M. Mostepanenko, *Physics reports* **353**, 1 (2001).
 [11] G. Plunien, B. Müller, and W. Greiner, *Physics Reports* **134**, 87 (1986).
 [12] J. N. Munday, F. Capasso, and V. A. Parsegian, *Nature* **457**, 170 (2009).
 [13] O. Kenneth, I. Klich, A. Mann, and M. Revzen, *Physical review letters* **89**, 033001 (2002).
 [14] R. Zhao, J. Zhou, T. Koschny, E. Economou, and C. Soukoulis, *Physical review letters* **103**, 103602 (2009).
 [15] G. T. Moore, *Journal of Mathematical Physics* **11**, 2679 (1970).
 [16] M. F. Maghrebi, R. L. Jaffe, and M. Kardar, *Physical review letters* **108**, 230403 (2012).
 [17] R. W. Boyd, *Nonlinear optics* (Academic press, 2019).
 [18] E. Yablonovitch, *Physical Review Letters* **62**, 1742 (1989).
 [19] L. C. Crispino, A. Higuchi, and G. E. Matsas, *Reviews of Modern Physics* **80**, 787 (2008).
 [20] S. A. Fulling and P. C. Davies, *Proceedings of the Royal Society of London. A. Mathematical and Physical Sciences* **348**, 393 (1976).
 [21] W. G. Unruh and R. M. Wald, *Physical Review D* **29**, 1047 (1984).
 [22] S. W. Hawking, *Communications in mathematical physics* **43**, 199 (1975).
 [23] W. G. Unruh, *Physical Review D* **14**, 870 (1976).
 [24] Y. Shtanov, J. Traschen, and R. Brandenberger, *Physical Review D* **51**, 5438 (1995).
 [25] P. Nation, J. Johansson, M. Blencowe, and F. Nori, *Reviews of Modern Physics* **84**, 1 (2012).
 [26] R. J. Glauber and M. Lewenstein, *Physical Review A* **43**, 467 (1991).
 [27] D. F. Walls and G. J. Milburn, *Quantum optics* (Springer Science & Business Media, 2007).
 [28] M. O. Scully and M. S. Zubairy, *Quantum optics* (1999).
 [29] R. Loudon and P. L. Knight, *Journal of modern optics* **34**, 709 (1987).
 [30] G. Breitenbach, S. Schiller, and J. Mlynek, *Nature* **387**, 471 (1997).
 [31] T. C. Ralph and P. K. Lam, *Physical review letters* **81**, 5668 (1998).
 [32] E. Polzik, J. Carri, and H. Kimble, *Physical review letters* **68**, 3020 (1992).
 [33] J. Aasi, J. Abadie, B. Abbott, R. Abbott, T. Abbott, M. Abernathy, C. Adams, T. Adams, P. Addesso, R. Adhikari, et al., *Nature Photonics* **7**, 613 (2013).
 [34] C. M. Wilson, G. Johansson, A. Pourkabirian, M. Simoen, J. R. Johansson, T. Duty, F. Nori, and P. Delsing, *Nature* **479**, 376 (2011).
 [35] A. W. Rodriguez, F. Capasso, and S. G. Johnson, *Nature photonics* **5**, 211 (2011).
 [36] A. Volokitin and B. N. Persson, *Reviews of Modern Physics* **79**, 1291 (2007).
 [37] V. Dodonov, *Physica Scripta* **82**, 038105 (2010).
 [38] C. Law, *Physical Review A* **49**, 433 (1994).
 [39] E. Lustig, Y. Sharabi, and M. Segev, *Optica* **5**, 1390 (2018).
 [40] J. R. Zurita-Sánchez, P. Halevi, and J. C. Cervantes-Gonzalez, *Physical Review A* **79**, 053821 (2009).
 [41] R. Chu and T. Tamir, in *Proceedings of the Institution of Electrical Engineers* (IET, 1972), vol. 119, pp. 797–806.
 [42] F. Harfoush and A. Taflove, *IEEE transactions on antennas and propagation* **39**, 898 (1991).
 [43] R. Fante, *IEEE Transactions on Antennas and Propagation* **19**, 417 (1971).
 [44] D. Holberg and K. Kunz, *IEEE Transactions on Antennas and Propagation* **14**, 183 (1966).
 [45] S. Scheel and S. Y. Buhmann, *Acta physica slovacica* **58.5**, 675 (2008).
 [46] N. Rivera and I. Kaminer, *Nature Reviews Physics* **2**, 538 (2020).
 [47] R. Schützhold, G. Plunien, and G. Soff, *Physical Review A* **58**, 1783 (1998).
 [48] F. Belgiorno, S. Cacciatori, G. Ortenzi, V. Sala, and D. Faccio, *Physical review letters* **104**, 140403 (2010).
 [49] S. Scheel and D.-G. Welsch, *Physical review letters* **96**, 073601 (2006).
 [50] J. Crosse and S. Scheel, *Physical Review A* **81**, 033815 (2010).
 [51] F. Lindel, R. Bennett, and S. Y. Buhmann, *Physical Review A* **103**, 033705 (2021).
 [52] J. Chen, M. Badioli, P. Alonso-González, S. Thongrattanasiri,

- F. Huth, J. Osmond, M. Spasenović, A. Centeno, A. Pesquera, P. Godignon, et al., *Nature* **487**, 77 (2012).
- [53] S. Dai, Z. Fei, Q. Ma, A. Rodin, M. Wagner, A. McLeod, M. Liu, W. Gannett, W. Regan, K. Watanabe, et al., *Science* **343**, 1125 (2014).
- [54] S. Dai, Q. Ma, M. Liu, T. Andersen, Z. Fei, M. Goldflam, M. Wagner, K. Watanabe, T. Taniguchi, M. Thiemens, et al., *Nature nanotechnology* **10**, 682 (2015).
- [55] D. Basov, M. Fogler, and F. G. De Abajo, *Science* **354**, aag1992 (2016).
- [56] A. Cartella, T. F. Nova, M. Fechner, R. Merlin, and A. Cavalleri, *Proceedings of the National Academy of Sciences* **115**, 12148 (2018).
- [57] J. Le Gall, M. Olivier, and J.-J. Greffet, *Physical Review B* **55**, 10105 (1997).
- [58] A. Woessner, M. B. Lundeberg, Y. Gao, A. Principi, P. Alonso-González, M. Carrega, K. Watanabe, T. Taniguchi, G. Vignale, M. Polini, et al., *Nature materials* **14**, 421 (2015).
- [59] Y. Cai, L. Zhang, Q. Zeng, L. Cheng, and Y. Xu, *Solid state communications* **141**, 262 (2007).
- [60] F. H. Koppens, D. E. Chang, and F. J. Garcia de Abajo, *Nano letters* **11**, 3370 (2011).
- [61] M. Jablan, H. Buljan, and M. Soljačić, *Physical review B* **80**, 245435 (2009).
- [62] T. Christensen, *From classical to quantum plasmonics in three and two dimensions* (Springer, 2017).
- [63] M. Bock, A. Lenhard, C. Chunnillall, and C. Becher, *Optics express* **24**, 23992 (2016).
- [64] M. Mitrano, A. Cantaluppi, D. Nicoletti, S. Kaiser, A. Perucchi, S. Lupi, P. Di Pietro, D. Pontiroli, M. Riccò, S. R. Clark, et al., *Nature* **530**, 461 (2016).
- [65] M. Babadi, M. Knap, I. Martin, G. Refael, and E. Demler, *Physical Review B* **96**, 014512 (2017).
- [66] L. Novotny and B. Hecht, *Principles of nano-optics* (Cambridge university press, 2012).
- [67] The two Fourier transforms are defined with opposing sign conventions so that for a time-independent material, $\chi(\omega, \omega') = 2\pi\delta(\omega - \omega')\chi(\omega)$.
- [68] For an isotropic layer of thickness d , the reflection coefficient is given as $r_p(\omega, q) = (r_{12} + r_{23}e^{2ik_{2z}d})/(1 - r_{21}r_{23}e^{2ik_{2z}d})$. Here $r_{ij} = \frac{\varepsilon_j k_{iz} - \varepsilon_i k_{jz}}{\varepsilon_j k_{iz} + \varepsilon_i k_{jz}}$ is the reflection coefficient between layer i and j , ε_i is the permittivity of the i -th layer (numbered from top to bottom in the z direction), and $k_{iz} = \sqrt{\frac{\omega^2}{c^2}\varepsilon_i - q^2}$ [66].